Band structure of silicon as measured in extended momentum space

M. Vos, C. Bowles, A. S. Kheifets, and M. R. Went

Atomic and Molecular Physics Laboratory, Research School of Physical Sciences and Engineering,
The Australian National University, Canberra ACT 0200, Australia

Direct measurement of the wave function (or at least the modulus squared of the wave function, the spectral function) is an important goal in electron spectroscopy. This requires a state-selective (i.e., energy resolved) measurement of the momentum density in all of momentum space, not just the reduced Brillouin zone. Photoemission has been used very successfully to measure dispersion, mainly in the reduced zone scheme. Compton measurements determine a projection of the momentum density in the full momentum space, but do not contain energy information. Here we present electron momentum spectroscopy measurements of extremely thin silicon single crystals, that resolve both energy and momentum, not just the reduced momentum. Measurements were done along different lines in extended momentum space, that are equivalent within the reduced zone scheme. For different lines different bands dominate, resulting in dramatic different spectral momentum densities. The observed intensities compare well to the spectral function as obtained by linear muffin tin band structure calculations. The results show a unified picture that forms a bridge between Compton measurements determining densities and photoemission measurements determining dispersion.

I. INTRODUCTION

There are two rather different approaches to the study of the electronic structure of matter. One approach, the oldest,[1] is Compton scattering, and it aims to determine the momentum densities.[2] In a Compton scattering experiment an incoming particle (usually a photon with keV energy) is detected after scattering over a large angle from a target electron. The energy of the scattered photon contains information about a momentum component of the electron it scattered from. For a free electron metal the valence band resembles a sphere in momentum space with radius $\mathbf{k}_f$, the Fermi momentum. Within this sphere the momentum density is constant, outside the sphere it is zero. For a correlated electron gas the sudden drop in intensity at $\mathbf{k}_f$ is reduced due to electron-electron interactions. Also, additional structures appear due to the lattice potential. As this technique does not resolve binding energy, it measures a projection of the momentum density integrated over all occupied states (both valence and core states). The full three-dimensional momentum density can be reconstructed from the result of Compton measurements for different crystal orientations.

A second technique, that has dominated the research of the electronic structure in recent decades, is angular-resolved photoemission.[3] It is used to measure, with great accuracy, the band dispersion, i.e., the binding energy of the Bloch waves as a function of the reduced momentum $\mathbf{k}$. The Bloch wave $\psi_\mathbf{k}$ is defined as

$$\psi_\mathbf{k}(\mathbf{r}) = \sum_\mathbf{G} c_{\mathbf{k}-\mathbf{G}} e^{i(\mathbf{k}-\mathbf{G})\cdot\mathbf{r}} \qquad (1)$$

with the summation extending over all reciprocal lattice vectors $\mathbf{G}$. The momentum density is thus equal to $|c_{\mathbf{k}-\mathbf{G}}|^2$ at $\mathbf{k}=\mathbf{G}$ and zero for all other momentum values. Thus knowledge of the (modulus square of the) coefficients $c_{\mathbf{k}-\mathbf{G}}$ is required to obtain the momentum density of the Bloch wave.

This information is difficult to obtain from the photoemission measurement. Hence in almost all cases interpretation of photoemission data is restricted to comparing observed and calculated dispersion in the reduced zone scheme.

There is very little comparison possible between the outcome of both techniques, each can be compared to theoretical calculations, but a Compton profile by itself does not contain information about dispersion, and a dispersion measurement does not easily help interpreting Compton profiles. Electron momentum spectroscopy (EMS) relies just as Compton scattering experiments on impulsive collisions of the incoming projectile with a target electron,[4] and it is able to resolve dispersion. EMS provides thus an experimental link between Compton and photoemission research. Here we want to demonstrate, using the case of silicon as an example, that a more complete picture emerges, if momentum densities and dispersion are measured simultaneously.

EMS is an (e,2e) experiment in the high energy limit, where the plain-wave impulse approximation is valid. In EMS the observed intensity can be directly compared to the electronic structure. It can be applied to atoms and (organic) molecules in the gas phase (see, e.g., Ref. 5 for a recent example). Interesting low energy (e,2e) experiments, done in a reflection geometry from surfaces (see, e.g., Ref. 6), are not in the high-energy limit, and their interpretation is more involved.

This paper is part of an ongoing project of determining what aspects of the band structure and momentum densities can be measured by EMS, using silicon as an example. We have investigated in previous works the dispersion along the main symmetry directions,[7] the influence of sample rotations on the measured spectral momentum densities,[8] and the possibility of measuring momentum densities along lines in momentum space, not going through zero momentum.[9] This last option is investigated in this paper in more detail. We measure in a systematic way the momentum densities along lines in momentum space that are separated by a reciprocal lattice
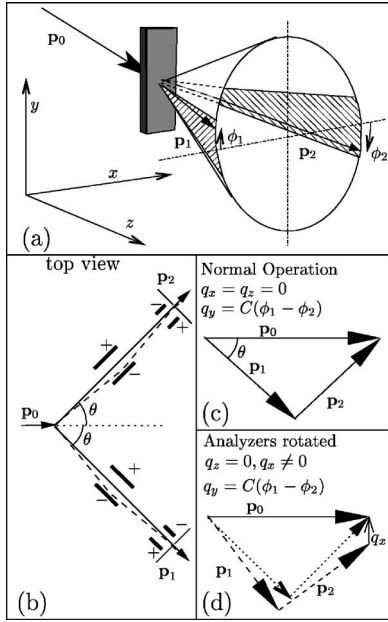
FIG. 1. The EMS spectrometer and the working of its deflectors. In (a) we show the geometry of the experiment. Scattered and ejected electrons with momenta in the hatched area are detected. In (b) we show the top view (looking down along the *y*-axis) with the scattering angle θ that can be varied by two sets of deflectors (dashed lines are trajectories with deflectors switched on). In (c) we show that the scattering angle θ is chosen in such a way that the recoil momentum is along the *y*-axis and proportional to $\phi_1 - \phi_2$. By applying voltages to the deflectors one can change the scattering angle and measure also the momentum densities for momentum values with either one or both components of $q_{x,z} \neq 0$ (d).

vector. In the reduced zone scheme all these measurements are equivalent. For a given momentum value peaks in the spectra are only observed at the energies of the bands at this momentum value. The relative amount by which each band contribute changes dramatically, if we shift the measurement by a reciprocal lattice vector, in a way that reflects the momentum density and thus revealing new and important information about the (modulus square of) coefficients $|c_{\mathbf{k-G}}|^2$ of the Bloch function. Thus the focus of this paper is to see if measured values of $|c_{\mathbf{k-G}}|^2$ resemble the calculated ones. It is an aspect of the electronic structure that has not been investigated in detail before.

II. EXPERIMENTAL DETAILS

In an EMS experiment a beam of well-collimated electrons with accurately known energies impinges on a thin film. Some of these electrons collide with a target electron and transfer a large fraction of their energy to those electrons. In our spectrometer, described extensively before,[10] the scattered and ejected electron are detected in coincidence and analyzed for their energy and momentum. EMS measurements are often referred to as "kinematically complete" as the energy and momentum of the incoming and both outgoing electrons are determined. Hence we can obtain the binding energy ε and momentum $\mathbf{q}$ of the ejected electron
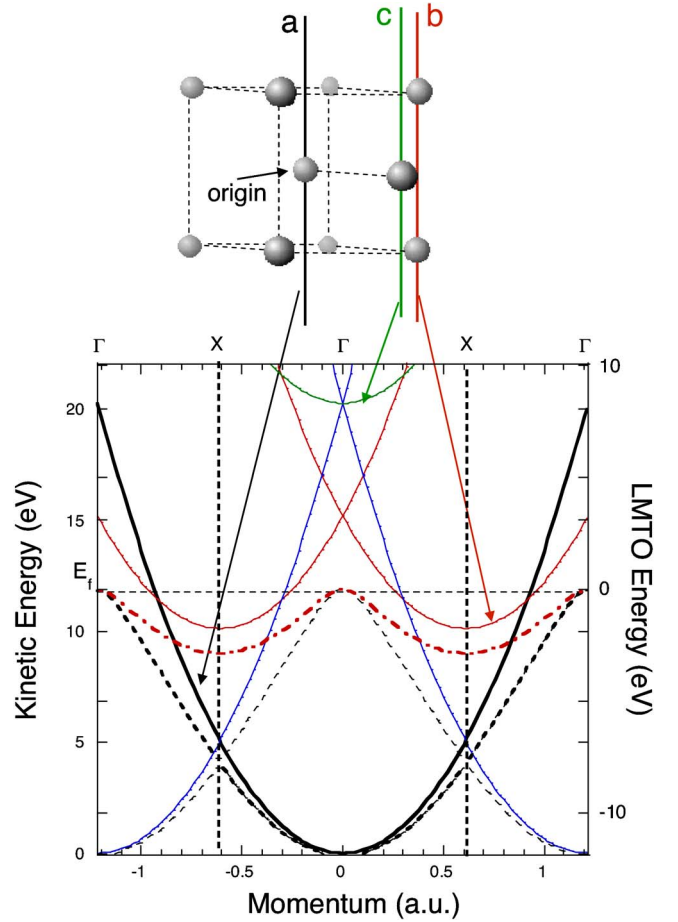

FIG. 2. (Color online) A comparison of the free electron band structure (full lines) and occupied part of the LMTO band structure of Si (dashed) plotted in the repeated zone scheme, for the $\langle 100 \rangle$ direction. Lines (b) and (c) can be obtained by shifting line (a) by a $\langle 111 \rangle$ or $\langle 200 \rangle$ type reciprocal lattice vector, and are hence equivalent in the repeated zone scheme. However, the kinetic energy in the free electron gas model is different along these three lines. Experimentally we measure these lines using the deflectors, by shifting line (a) by $\langle 101 \rangle$ or $\langle 200 \rangle$, respectively. As $\langle 101 \rangle$ is not a reciprocal lattice vector, we will measure in case (b) the Γ point not at $p_y = 0$, but at $p_y = 0.6$ a.u.

before the collision:

$$\varepsilon = E_0 - E_1 - E_2 \qquad (2)$$

$$\mathbf{q} = \mathbf{p}_1 + \mathbf{p}_2 - \mathbf{p}_0, \qquad (3)$$

with $E_{0,1,2}$ the energy of the incoming, scattered and ejected electron respectively, and $\mathbf{p}_{0,1,2}$ their momenta. These equations only apply if the collision with the target electron is the only interaction with the target. For gas-phase experiments at keV energies this assumption is usually well-justified, but for thin film experiments this becomes a reasonable approximation only when using extremely thin films (about 10 nm) and high energies (here 50 keV for the incoming, 25 keV for the outgoing electrons). A diffraction pattern could be recorded on a phosphorous screen behind the sample. It showed that
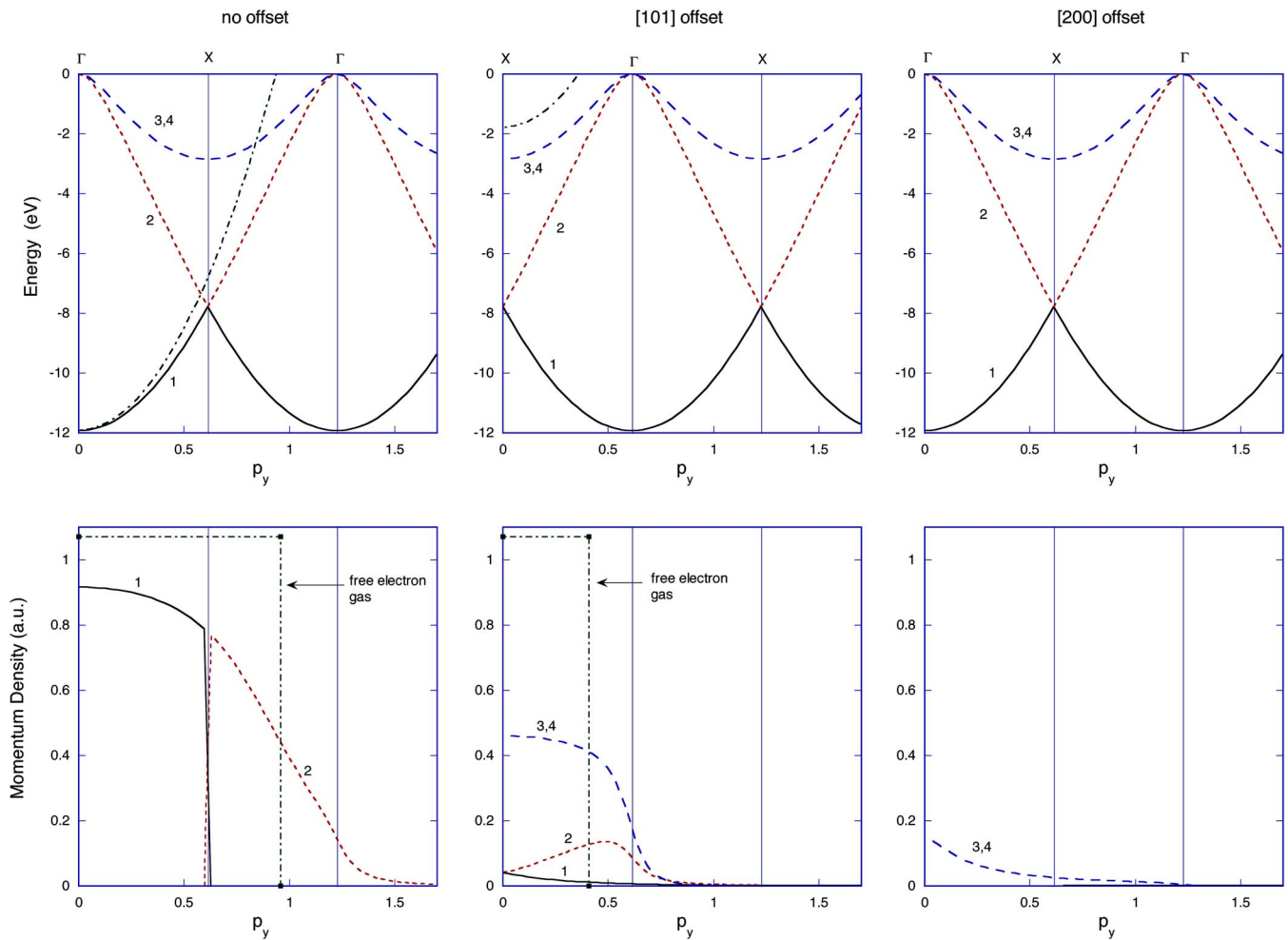
FIG. 3. (Color online) The calculated dispersion and momentum densities for the three lines shown in Fig. 2. The corresponding dispersion and momentum density of a free electron gas is indicated by a dashed-dotted line (density is zero for the case with a [200] offset).

the diffraction spots of the diffracted beams were much weaker than the spot of the primary beam.

Our spectrometer has a noncoplanar symmetric configuration (see Fig. 1). This means that the scattering angle of both detected electrons is identical ($\theta = 44.3°$), but the momentum of the ejected electron is not necessarily in the plane defined by the incoming and scattered momentum vectors. For 50 keV incoming and 25 keV outgoing electrons (and $\theta = 44.3°$) the recoil momentum is zero if all three trajectories are in the same plane ($\phi_1 = \phi_2$). If these trajectories are not in the same plane then (for the small range of ϕ values $\pm 6°$ that are covered by our analyzers), to a good approximation, the recoil momentum is directed along the spectrometer y-axis and its magnitude is proportional to $\phi_1 - \phi_2$.

Between the sample and each of the analyzers there is a double deflector. Applying voltages to the double deflector changes which electrons are detected by the detector: It effectively changes the scattering angle θ by up to $\pm 1.3°$. This is sketched in Fig. 1(b). Thus if, due to construction imperfections, the geometry without deflector voltages of coplanar events ($\phi_1 = \phi_2$) does not correspond to $q = 0$ we can use the deflectors to effectively change the collision geometry in such a way that $q_x = 0$ and $q_z = 0$. The value $q_y = 0$ is always

included, due to the use of analyzers that measure simultaneously a range of ϕ angles. The offset component q_y can thus be determined directly as the observed intensity distribution should be symmetrical around $q_y = 0$.

In this paper we investigate silicon single crystal samples. Sample preparation techniques used were described by Utteridge *et al.*[11] If we, for example, align the y-axis of the spectrometer with the sample $\langle 010 \rangle$ direction we measure the dispersion and momentum density along the p_y axis ($p_x = 0$, $p_z = 0$), i.e., Γ-X direction. Usually the electronic structure is plotted in the reduced zone scheme. In this presentation all lines in momentum space than can be reached by shifting the p_y axis by a reciprocal lattice vector are equivalent. We can measure along these equivalent lines by introducing an offset in the measurement using the deflectors. If the shift corresponds to a reciprocal lattice vector that is perpendicular to the p_y axis then the measurement at $p_y = 0$ corresponds again to a reciprocal lattice point, usually referred to as a Γ point.

Often the reciprocal lattice vector has a component along the p_y-direction. The deflectors have only effect in the p_x-p_z plane. In that case the measurement at $p_y = 0$ will not correspond to a Γ point but the Γ point will be reached for p_y values corresponding to the p_y component of the reciprocal lattice vector.

Note that if we apply deflector voltages such that ($p_x \neq 0$ or $p_z \neq 0$), the measurement is along a line with a fixed offset, and variable p_y magnitude. Thus such a measurement does *not* correspond to a measurement along a specific direction, but should be visualized as a line in momentum space, that does not intersect the origin.

III. DISPERSION AND MOMENTUM DENSITIES

The approach used in EMS differs from the usual studies of the electronic structure of matter. Here we want to explain in simple terms how momentum densities and dispersion are related, by considering the electronic structure of silicon as a free-electron gas perturbed by a lattice potential. Thus first we consider a free electron material with the same electron density as Si, subsequently consider the potential as a perturbation, and compare this with the actual linear muffin-tin orbital (LMTO) calculation.[12] We summarize it here to stress the importance of the fundamental properties we want to measure, that are theoretically well established but until now elude *direct* experimental observations. We do not elaborate on other aspects of the electronic structure of Si, including many-body effects, which are discussed extensively elsewhere.[7]

Silicon has a valence electron density of $0.030e^-$/a.u.^{3} (we will work mainly in atomic units, this density corresponds to 0.20 e$^-$/Å^3, 1 a.u. of momentum$=1.89$ Å^{-1}). A free electron solid with the same density would have occupied states within a radius of $k_f=0.96$ a.u. (1.8 Å^{-1}). The total occupied band width of a free electron solid with this density is 11.7 eV.

Inside the Fermi sphere there is a constant momentum density, as the allowed k values are determined by the boundary conditions. For a cubic volume with side L the separation is $2\pi/L$. Thus the momentum density is $\rho=[L/(2\pi)]^3$ and depends on the size of the sample. In calculations the momentum density is usually given normalized to a single unit cell volume. For a free electron solid with the same unit cell volume as silicon the momentum density would be 1.09 a.u.^{3}.

Consider now an EMS measurement of this free electron gas. If we use the deflectors in such a way that we measure along a line that intersects zero momentum (by applying small voltages, correcting for spectrometer imperfections, residual magnetic fields[9]), then, for a free electron solid, we measure the total width of the occupied free-electron band. The binding energy is determined by the potential energy of the free electron material V_0 and its kinetic energy $E_{kin}=(\hbar q)^2/2m_e$ which simplifies to $q^2/2$ in atomic units. The maximum binding energy is thus at $\mathbf{q}_y=0$ and the minimum binding energy (Fermi level) is observed for $|q_y|=k_f$. The measured intensity would be along the thick line in Fig. 2. Changing the deflectors setting so we measure along a line that crosses the q_x,q_z plane at a distance Δq_{xz} from the origin will cause the maximum binding energy observed to decrease by $\Delta q_{xz}^2/2$. The maximum momentum for which intensity is observed (again at the Fermi level) is now the q_y value for which $q_y^2+\Delta q_{xz}^2=k_f^2$, thus the width (in terms of momentum and energy) of the observed parabola decreases with increasing Δq_{xz}.

Now we turn on the crystal lattice, and first consider it as a small perturbation. Two points that are now separated by a reciprocal lattice vector are considered equivalent in the reduced zone scheme. We want to compare EMS measurements along the lines in momentum space that are separated by reciprocal lattice vectors. The shortest reciprocal lattice vector for silicon (which has a BCC reciprocal lattice) is ⟨111⟩, followed by ⟨200⟩. In Fig. 2 (top) we show such a shifted line. We can measure this line again if we apply voltages to the deflector in such a way that $\Delta q_x=\Delta q_z=0.61$ a.u. Note that $q_y=0$ now does not correspond to a reciprocal lattice point, but corresponds to ⟨101⟩ a symmetry point that is usually referred to as an X point. Thus, as long as the effect of the lattice potential is small we expect to measure again a parabola. It has its maximum binding energy at ⟨101⟩, an X point rather than at a Γ point. If we plot this line in the band structure plot it would correspond to the thin full line, highlighted by an arrow in Fig. 2.

Now consider the true potential of a silicon crystal. The dispersion is now obtained from a full potential LMTO calculation, and is shown by dashed lines and dashed-dotted lines in Fig. 2. It deviates substantially from the free electron model. However, the underlying free electron band structure can still be recognized. The thick dashed line follows for small momenta the free electron band closely. Hence we ex-
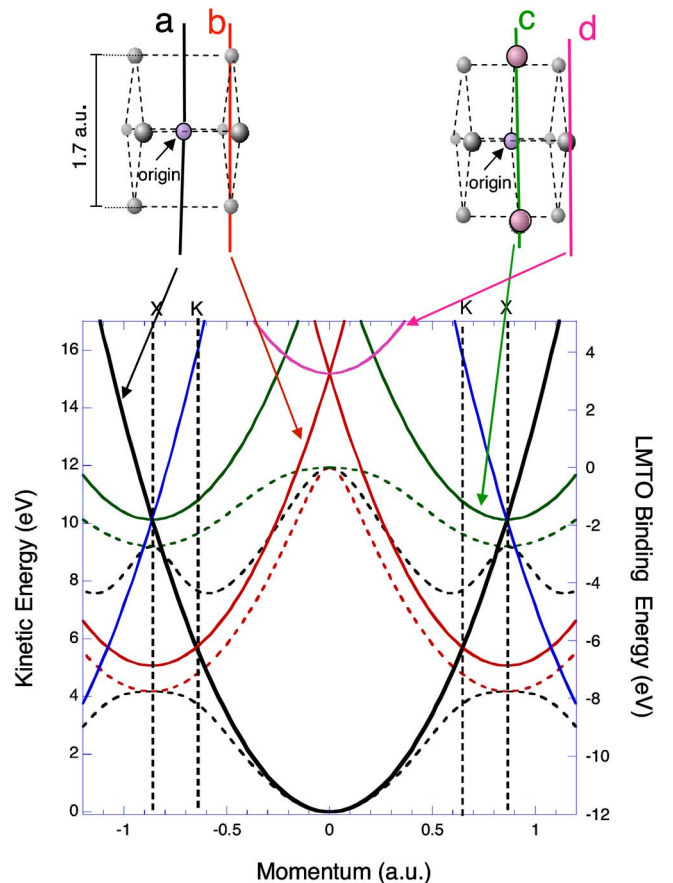

FIG. 4. (Color online) A comparison of the free electron band structure and LMTO band structure for the different measurements for the Γ-K-X measurement. Lines (b)–(d) are obtained by shifting line (a) by [001], [1$\bar{1}$0], and [1$\bar{1}$1], respectively.

pect to measure this band if we measure along a line through zero momentum. If we measure along a line shifted by $\langle 101 \rangle$ then we expect intensity along the dashed-dotted (red) line, as it follows the shifted free electron parabola. Near the Γ point, reached for the $\langle 101 \rangle$ shifted line at $q_y = 0.61$ a.u., there are substantial deviations of the LMTO calculations from the free electron band and hence we expect to find experimentally rather different intensities than predicted by the free electron band model, as here the lattice potential causes a strong mixing of the wave function.

Comparison of the experiment with theory is easier if we plot the dispersion and intensities in momentum space (extended zone scheme) as a function of q_y. This is done in Fig. 3 for the standard measurement (through zero momentum) and measurement shifted by $\langle 101 \rangle$ and $\langle 200 \rangle$. In the second case $q_y = 0$ correspond to an X point, whereas the first and last ones $q_y = 0$ correspond to the Γ point. The momentum densities are always lower than those predicted by the free electron model. This is attributed to the fact that in silicon the valence wave functions are orthogonalized to the core wave function. This introduces a rapidly oscillating behavior in the wave function near the nuclei, corresponding to a high momentum component, and hence reduces the density at low momentum values. However, our conclusion, based on the free electron model, that for $\Delta q_{xz} = 0$, bands 1 and 2 dominate, and for the $\Delta q_{xz} = [101]$ bands 3 and 4 dominate, is corroborated by the LMTO calculation. If we apply voltages

such that $\Delta q_{xz} = [200]$, then the line along which we measure is always well outside the Fermi sphere. Hence only relative small densities are expected, and indeed the LMTO calculation shows only minor densities in bands 3 and 4 near $q_y = 0$. The calculated density and energy at $\Delta q_{xz} = [000]$, $q_y = 1.2$ a.u. is equal to those at $\Delta q_{xz} = [200]$, $q_y = 0$ as these points correspond to $\Gamma_{\langle 200 \rangle}$ and $\Gamma_{\langle 020 \rangle}$, respectively, equivalent points for a cubic lattice. In the first case increasing q_y will cause intensity along band 2, in the second case along bands 3 and 4.

By rotating the crystal over 45° along the surface normal we can align the $\langle 110 \rangle$ symmetry (the Γ-K direction) direction with the spectrometer y-axis. In this direction the dispersion shows 4 bands, and because of the somewhat lower symmetry we can measure the spectral momentum density for 3 inequivalent shifts of the measurement line away from the origin. The relation between the shifts, free electron dispersion and actual LMTO dispersion is emphasized in Fig. 4. Now the x-, y-, and z-axis of the spectrometer coincide with the $\langle 1\bar{1}0 \rangle$, $\langle 110 \rangle$, and $\langle 001 \rangle$ crystallographic directions, respectively. The shifts introduced by the deflectors are now $[001]$, $[1\bar{1}0]$, and $[111]$. For the first two shifts $q_y = 0$ corresponds again to an X point (the $[001]$ and $[1\bar{1}0]$ points are separated by $[\bar{1}11]$, a reciprocal lattice vector, and are hence both points are equivalent in the reduced zone scheme).
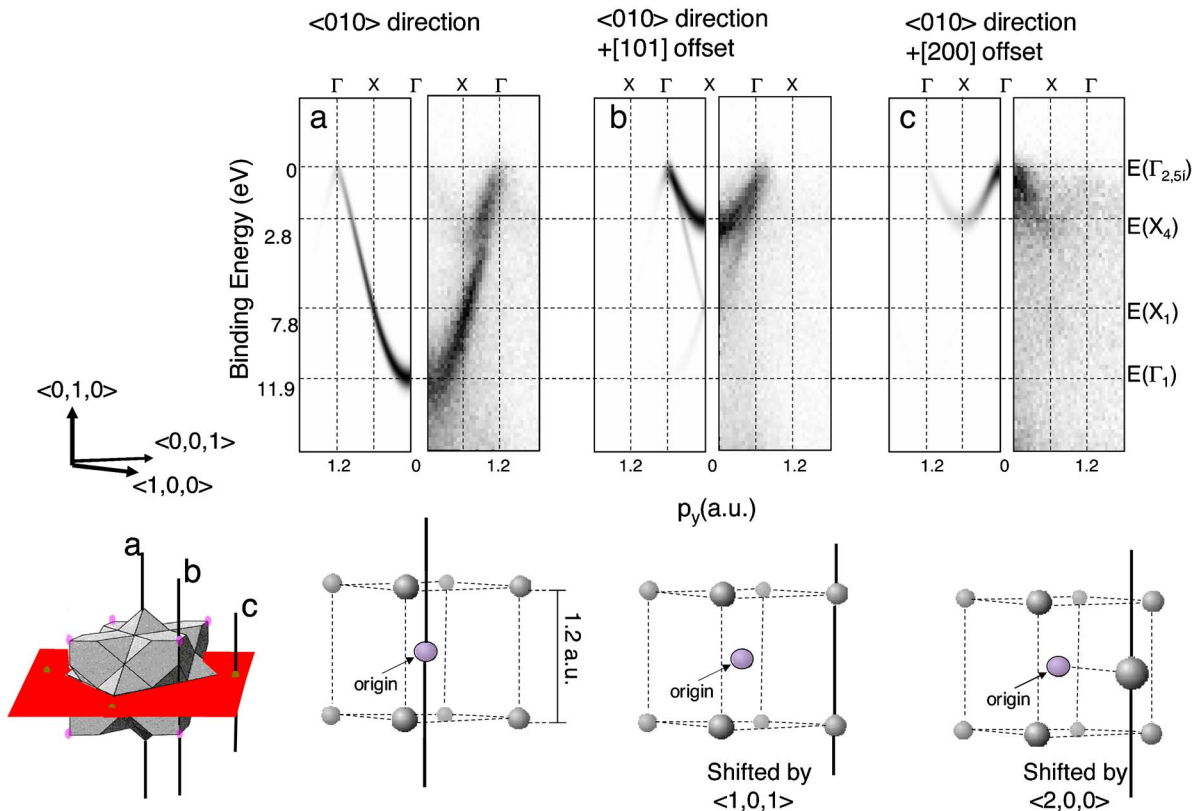

FIG. 5. (Color online) Measurements (right halves) and calculated (left halves) spectral momentum densities along different lines along the Γ-X directions. Each plot is normalized so the highest intensity corresponds to black. In the bottom half we indicate the position of the measurement lines in the reciprocal lattice. In the bottom left we show a picture of the second Brillouin zone together with the three measurement directions.
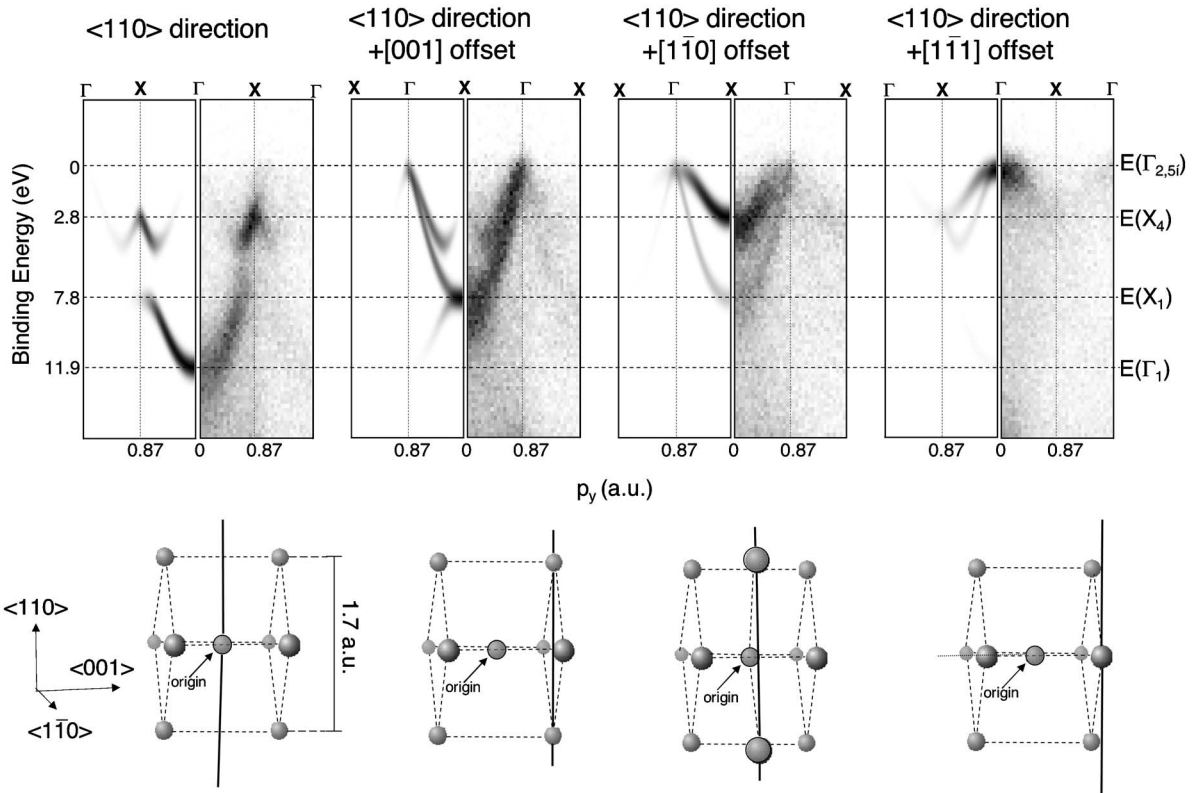
FIG. 6. Similar plots as Fig. 5, but now for measurements along Γ-K-X lines.

IV. EXPERIMENTAL RESULTS

Now let us compare the actual EMS measurements with LMTO calculations for three measurements of Γ-X lines (Fig. 5). In these measurements we used the procedure described in Ref. 8 to minimize the influence of diffraction. At first glance, the three experimental measurements seem completely different, but closer inspection and a comparison with

Fig. 3 reveals that the calculated intensities are well reproduced in the experiment. For the measurement through zero momentum we see that bands 1 and 2 dominate. For measurements shifted by [110] bands 3 and 4 dominate but traces of band 2 can be seen in both theory and experiment. Finally if we apply voltages to the deflectors corresponding to a shift of the measurement line by [200] (a reciprocal lattice vector)
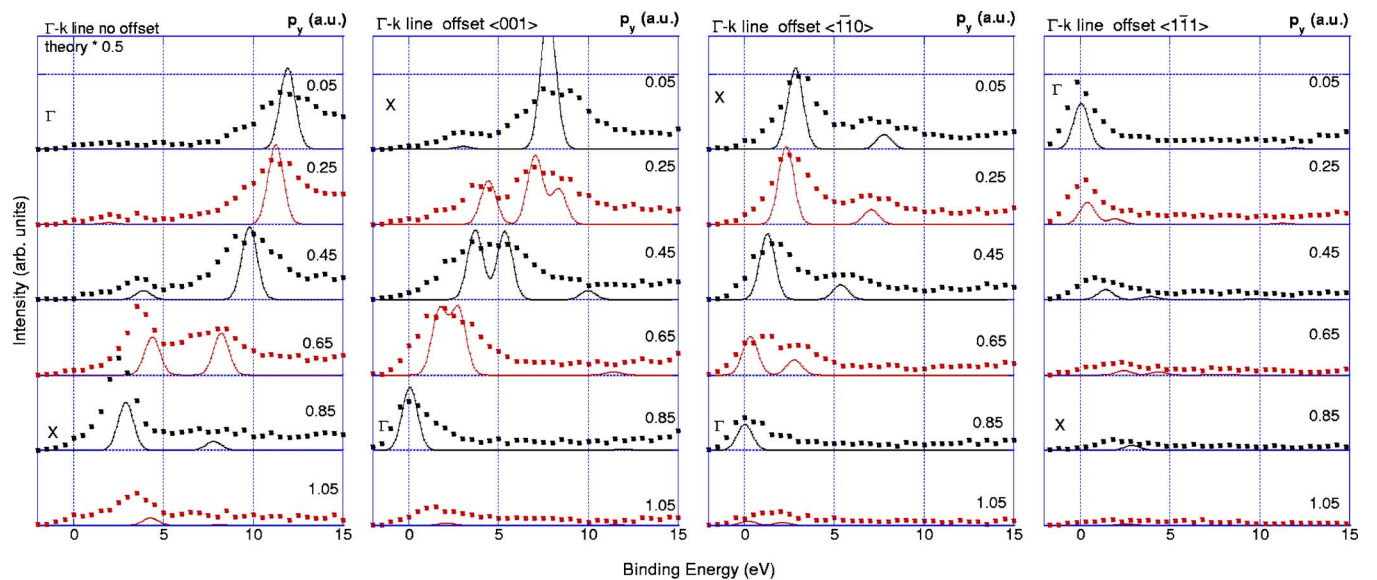

FIG. 7. (Color online) Measured intensity (dots) along various Γ-K-X lines compared with the LMTO calculations. All plots have the same normalization, except the LMTO graphs in the left-most panel, for which the height is reduced by a factor of 2.

TABLE I. The momentum density of the inner and outer valence band at the innermost Γ points.

Γ_{xyz}	$\lvert q \rvert$	$\rho \, (\Gamma_1)$	$\rho \, (\Gamma_{2,5'})$
$\langle 000 \rangle$	0	0.92	0
$\langle 111 \rangle$	1.06	6.7×10^{-3}	0.27
$\langle 200 \rangle$	1.22	0	0.15
$\langle 220 \rangle$	1.73	1.5×10^{-3}	3.2×10^{-3}

we measure again a Γ point at $p_y=0$ and intensity corresponds to the top of the valence band. Increasing $p_y=0$ shows an increase in binding energy, in spite of the fact that the magnitude of the momentum (and hence kinetic energy) increases with p_y. Thus here the influence of the lattice potential dominates the dispersion behavior.

Thus a large variety in spectral momentum distributions is obtained, as the main intensity is concentrated along lines that follow the dispersion of the bands. In first approximation the momentum values for which there is a large intensity can be obtained by considering the intensity as would be obtained for a free electron gas. However, especially near the Brillouin zone boundaries there are significant deviations. The agreement between the LMTO theory (see also Fig. 3) and experiment is satisfactorily, considering the level of multiple scattering in the experiment.

For a more quantitative comparison we plot in Figs. 6 and 7 the spectra obtained for the Γ-K-X measurement. This set of data is less affected by diffraction[9] and hence more suitable for quantitative analysis. For the deepest part of the valence band life time broadening is significant, hence the calculated spectra are much sharper and higher near the bottom of the band compared to the observed ones. This variation in width makes quantitative comparison of the intensity at the bottom and top of the band difficult. We want to focus here on the intensity at the top of the band. We have two measurements here of the intensity of $\Gamma_{2,5'}$. In the second panel we have an offset due to the deflectors of $\langle 001 \rangle$. At $p_y=0.86$ a.u. we have an offset along the Γ-K-X direction corresponding to $\langle 110 \rangle$, hence the measurement at $p_y=0.86$ corresponds to a $\langle 111 \rangle$ reciprocal lattice point. For the measurement with a $\langle 1\bar{1}0 \rangle$ offset (third panel) we reach the $\langle 200 \rangle$ reciprocal lattice point when p_y corresponds to $\langle 110 \rangle$. Finally for the last measurement we have an offset of $\langle 1\bar{1}1 \rangle$ due to the deflectors and hence $p_y=0$ corresponds to a $\langle 1\bar{1}1 \rangle$ reciprocal lattice point. All four spectra are obtained in a single four day run, with the deflector voltages changing every minute under computer control. Thus the intensity of each of the four measurements can be compared to each other. The theory predicts that the occupation at $\Gamma_{\langle 111 \rangle}$ is 0.55 times that of $\Gamma_{\langle 200 \rangle}$ (see Table I). The measurements seem to collaborate that. For a fully quantitative comparison the small diffraction effects have to be properly accounted for, which is beyond the scope of the current paper. The measurement at zero momentum ($p_y=0$, no offset) does not show a peak at the top of the valence band. Thus no contribution to the density of the outermost wave function at zero momentum ($\Gamma_{\langle 000 \rangle}$) is observed.

V. CONCLUSION

We measured the electronic structure of silicon in the extended zone scheme. Measurements taken at momenta that differ by a reciprocal lattice vector show peaks at similar energies, but completely different intensities. A simple free-electron model is useful to predict which part of the LMTO band structure gives intensity in a certain region of (extended) momentum space. On a semiquantitative level good agreement is found between measured intensities and those predicted by LMTO theory. In the calculation the intensity is equal to $\lvert c_{\mathbf{k}-\mathbf{G}} \rvert^2$. Hence we have shown here that EMS measurements contain direct information about these coefficients. In particular the measurements seem to corroborate that the wave function at the top of the valence band consists out of plane waves of type $\langle 111 \rangle$ and $\langle 200 \rangle$, the latter being smaller than the first.

In conclusion, we have demonstrated that we can measure dispersion and momentum densities simultaneously at least in a semiquantitative way, hence building a bridge between Compton scattering and photoemission experiments.

[1] J. Dumond, Rev. Mod. Phys. **5**, 1 (1933).

[2] M. J. Cooper, P. E. Mijnarends, N. Shiotani, N. Sakai, and A. Bansil, *X-Ray Compton Scattering* (Oxford University Press, New York, 2004).

[3] S. Hüfner, *Photoelectron Spectroscopy* (Springer, Berlin, 1995).

[4] E. Weigold and I. E. McCarthy, *Electron Momentum Spectroscopy* (Kluwer Academic/Plenum, New York, 1999).

[5] G. Q. Li, J. K. Deng, B. Li, X. G. Ren, and C. G. Ning, Phys. Rev. A **72**, 062716 (2005).

[6] F. O. Schumann, J. Kirschner, and J. Berakdar, Phys. Rev. Lett. **95**, 117601 (2005).

[7] A. S. Kheifets, V. A. Sashin, M. Vos, E. Weigold, and F. Aryasetiawan, Phys. Rev. B **68**, 233205 (2003).

[8] M. Vos, C. Bowles, A. S. Kheifets, V. A. Sashin, E. Weigold, and F. Aryasetiawan, J. Electron Spectrosc. Relat. Phenom. **137-40**, 629 (2004).

[9] M. Vos, V. Sashin, C. Bowles, A. Kheifets, and E. Weigold, J. Phys. Chem. Solids **65**, 2035 (2004).

[10] M. Vos, G. P. Cornish, and E. Weigold, Rev. Sci. Instrum. **71**, 3831 (2000).

[11] S. J. Utteridge, V. A. Sashin, S. A. Canney, M. J. Ford, Z. Fang, D. R. Oliver, M. Vos, and E. Weigold, Appl. Surf. Sci. **162-163**, 359 (2000).

[12] A. S. Kheifets, D. R. Lun, and S. Y. Savrasov, J. Phys.: Condens. Matter **11**, 6779 (1999).